Dynamics of Calcium Sparks and Calcium Leak in the Heart

George S. B. Williams,[†‡] Aristide C. Chikando,[†‡] Hoang-Trong M. Tuan,[‡] Eric A. Sobie,[§] W. J. Lederer,[†] and M. Saleet Jafri[†‡]

[†]BioMET, University of Maryland, Baltimore, Baltimore, Maryland; [‡]School of Systems Biology, George Mason University, Fairfax, Virginia; and [§]Department of Pharmacology, The Mount Sinai School of Medicine, New York, New York

Supporting Material

Tables

Parameter	Definition	Value
V_{cell}	Cell volume	36.8 pL
V_{myo}	Myoplasmic volume	25.84 pL
λ_{nsr}	NSR volume fraction	0.0458
λ_{jsr}	JSR volume fraction	0.0130
λ_{ds}	Subspace volume fraction	1.55×10^{-04}
N	Number of CRUs	20,000
N_{ryr}	Number of RyRs per CRU	49
$[Ca^{2+}]_o$	Extracellular $[Ca^{2+}]$	1.8 mM
$[Na^{+}]_i$	Intracellular $[Na^{+}]$	10.2 mM
$[Na^{+}]_o$	Extracellular $[Na^{+}]$	140 mM
β_{ds}	Subspace Ca^{2+} buffering fraction	0.1
β_{nsr}	NSR Ca^{2+} buffering fraction	1
v_{ryr}^{T}	RyR Ca^{2+} release rate	4.9194e-05 s^{-1}
$v_{ryr,nj}$	Rogue RyR release rate	2.41 s^{-1}
η	Cooperativity of Ca^{2+} binding to RyR	2.2
a_*	Average RyR allosteric connectivity	0.07
ε_{cc}	Change in free energy between closed RyR pairs	-0.92 k_BT
ε_{oo}	Change in free energy between open RyR pairs	-0.85 k_BT

Table S1: Model Parameters

Parameter	Definition	Value
A_p	Concentration of SERCA molecules	150 μM
$K_{d,i}$	SERCA $[Ca^{2+}]_i$ sensitivity	0.91 mM
$K_{d,sr}$	SERCA $[Ca^{2+}]_{sr}$ sensitivity	2.24 mM
B^T_{myo}	Total myoplasmic Ca^{2+} buffer concentration	143 μM
K^{myo}_m	Half saturation constant for myoplasmic Ca^{2+} buffer	0.96μM
B^T_{jsr}	Total JSR Ca^{2+} buffer concentration	140×10^2 μM
K^{jsr}_m	Half saturation constant for JSR Ca^{2+} buffer	638μM
F	Faraday constant	9.6485×10^4 coul μmol
T	Temperature	310 K
R	Ideal gas constant	8314 J mM^{-1} K^{-1}
$\bar{I}_{pmca}$	Maximal PMCA current	0.75 pA pF^{-1}
K_{pmca}	Ca^{2+} half saturation constant for PMCA	0.5 μM
$\bar{I}_{ncx}$	Maximal NCX current	1000 pA pF^{-1}
g_{bca}	Maximal backgroung Ca^{2+} conductance	7.36351×10^{-4} mS μF
v^T_{refill}	Total JSR refill rate	5 s^{-1}
v^T_{efflux}	Total rate of Ca^{2+} efflux out of the susbspace	250 s^{-1}
k^+	RyR Ca^{2+} association rate constant	12 $\mu M^{-\eta}$ s^{-1}
k^-	RyR Ca^{2+} disassociation rate constant	500 s^{-1}
ϕ_m	Luminal Ca^{2+} regulation coefficient	2.3×10^{-4} μM^{-1}
ϕ_b	Luminal Ca^{2+} regulation coefficient	2.0×10^{-2}
η_{ncx}	NCX voltage dependence coefficient	0.35
$K_{ncx,ca}$	Ca^{2+} half saturation contant for NCX	1380 μM
$K_{ncx,na}$	Na^+ half saturation contant for NCX	87500 μM
k^{sat}_{ncx}	NCX exchange saturation factor	0.1
A_m	Capacitative area of cell membrane	1.5340×10^{-4} μF
V	Membrane voltage	-85 mV

Table S2: Model Parameters, cont.

Parameter	Definition	Value
$[Ca^{2+}]_i$	myoplasmic $[Ca^{2+}]$	90 nM
$[Ca^{2+}]_{ds}$	dyadic subspace $[Ca^{2+}]$	90 nM
$[Ca^{2+}]_{nsr}$	network SR $[Ca^{2+}]$	1 mM
$[Ca^{2+}]_{jsr}$	junctional SR $[Ca^{2+}]$	1 mM
$\pi^o_{ryr,nj}$	fraction of open "rogue" RyR	0

Table S3: Initial Conditions

Concentration Balance Equations

The Markov chain Monte Carlo model used here consists of 2N+2 (N = 20,000) ordinary differential equations (ODEs) representing the time-evolution of $[Ca^{2+}]$ in the bulk myoplasm ($[Ca^{2+}]_i$), NSR ($[Ca^{2+}]_{nsr}$), the N JSR ($[Ca^{2+}]_{jsr}$) and dyadic subspace ($[Ca^{2+}]_{ds}$) compartments, and N Markov chains representing the stochastic RyR clusters. Consistent with Fig. 1A, the concentration balance equations are

$$\frac{d[Ca^{2+}]_i}{dt} = \beta_{myo}\left(J^T_{efflux} - J_{ncx} - J_{serca} + J_{bca} - J_{pmca} + J_{ryr,nj}\right) \tag{S1}$$

$$\frac{d[Ca^{2+}]_{nsr}}{dt} = \frac{\beta_{nsr}}{\lambda_{nsr}}\left(J_{serca} - J^T_{refill} - J_{ryr,nj}\right) \tag{S2}$$

$$\frac{d[Ca^{2+}]^i_{jsr}}{dt} = \frac{\beta^i_{jsr}}{\lambda_{jsr}}\left(J^i_{refill} - J^i_{ryr}\right) \tag{S3}$$

$$\frac{d[Ca^{2+}]^i_{ds}}{dt} = \frac{\beta_{ds}}{\lambda_{ds}}\left(J^i_{ryr} - J^i_{efflux}\right) \tag{S4}$$

where λ_{nsr}, λ_{jsr}, and λ_{ds} are the fraction of myoplasmic volume for the NSR, JSR, and dyadic subspace, respectively. β_{ds} and β_{nsr} are constant fraction buffering constants for the dyadic subspace and NSR, respectively. β^i_{jsr} and β_{myo} are dynamic buffering fractions for the JSR and myoplasm, respectively (see Supporting Material). The superscript i in Eqs. S3 and S4 denotes the i-th subspace ($1 \leq i \leq N$). The flux through the RyR cluster associated with the i-th CRU is given by

$$J^i_{ryr} = N^i_o v_{ryr}\left([Ca^{2+}]^i_{jsr} - [Ca^{2+}]^i_{ds}\right) \tag{S5}$$

where v_{ryr} is the RyR Ca^{2+} release rate in s^{-1} and N^i_o is the number of open RyR channels at the i-th release site. Similar to previous work (24, 25) model parameters lead to rapid equilibrium of $[Ca^{2+}]_{ds}$ with the $[Ca^{2+}]_i$ and $[Ca^{2+}]_{jsr}$ allowing $[Ca^{2+}]_{ds}$ to be approximated using an algebraic expression of $[Ca^{2+}]_i$, $[Ca^{2+}]_{jsr}$, and N_o (see Eq. S23). The total Ca^{2+} flux from the NSR to JSR compartments and the total Ca^{2+} flux from the dyadic subspaces to the bulk myoplasm are given by J^T_{refill} and J^T_{efflux}, respectively.

Allosteric Coupling Formulation

Combining 49 identical two-state RyRs into a cluster and assuming they are instantaneously coupled via $[Ca^{2+}]_{ds}$ yields a M = 50 state release site where each state indicates the number of open RyRs (N_o) for the CRU ($0 \leq N_o \leq 49$) as shown in Fig. 1C where terms on the arrows are transition rates. In these rate terms, χ_{oc} and χ_{co} represent "mean-field" allosteric coupling factors (18) given by

$$\chi_{oc} = \exp\{-a_*[N_c\varepsilon_{cc} - (N_o - 1)\varepsilon_{oo}]\} \tag{S6}$$

$$\chi_{co} = \exp\{-a_*[N_o\varepsilon_{oo} - (N_c - 1)\varepsilon_{cc}]\} \tag{S7}$$

where a_* represents the average allosteric connectivity (based on a 7×7 grid with nearest neighbor coupling), ε_{cc} is a dimensionless free energy of interaction (units of k_BT) that specifies the change

in free energy experienced by a channel in state C when allosterically coupled to another channel in state C, and similarly for ε_{oo}. The coefficients N_c (number of closed RyRs) and N_o serve to partition allosteric coupling between the forward and reverse transitions.

Bulk Calcium Fluxes

The whole cell model of CICR that is the focus of this paper includes several fluxes that directly influence the dynamics of the bulk myoplasmic and NSR [Ca^{2+}] (see Eqs. S1 and S2) which, for brevity, are described below rather than in the text.

Sarcoplasmic/Endoplasmic Reticulum Ca^{2+}-ATPase

The sarcoplasmic/endoplasmic reticulum Ca^{2+}-ATPase (SERCA) consumes ATP to pump Ca^{2+} into the SR from the myoplasm. Tran and co-workers (21) developed a thermodynamically realistic formulation of the SERCA pump along with a simplified "two-state" formulation that is implemented here. The SERCA pump flux takes the form,

$$J_{serca} = 2v_{cycle}A_p \tag{S8}$$

where A_p is the concentration of SERCA molecules (μM) and v_{cycle} is the cycling rate (s^{-1}) per pump molecule, given by

$$v_{cycle} = \frac{3.24873\times10^{12}K_i{}^2 + K_i(9.17846\times10^6 - 11478.2K_{sr}) - 0.329904K_{sr}}{D_{cycle}} \tag{S9}$$

where

$$\begin{aligned} D_{cycle} =& 0.104217 + 17.923K_{sr} + K_i(1.75583\times10^6 + 7.61673\times10^6K_{sr}) + \\ & K_i{}^2(6.08463\times10^{11} + 4.50544\times10^{11}K_{sr}) \end{aligned}$$

and

$$K_i = \left(\frac{[Ca^{2+}]_i}{1\times10^{-3}K_{d,i}}\right)^2 \quad \text{and} \quad K_{sr} = \left(\frac{[Ca^{2+}]_{nsr}}{1\times10^{-3}K_{d,sr}}\right)^2$$

Na^+-Ca^{2+} Exchanger

The main pathway by which Ca^{2+} is extruded from the myocyte is the Na^+-Ca^{2+} exchanger (NCX) which can be described as

$$J_{ncx} = \frac{-A_m I_{ncx}}{FV_{myo}} \tag{S10}$$

$$I_{ncx} = \bar{I}_{ncx}\frac{[Na^+]_i^3[Ca^{2+}]_o e^{(\eta_{ncx}FV/RT)} - [Na^+]_o^3[Ca^{2+}]_i e^{(\eta_{ncx}-1)FV/RT}}{\left((K_{ncx,na})^3 + [Na^+]_o^3\right)(K_{ncx,ca} + [Ca^{2+}]_o)\left(1 + k_{ncx}^{sat}e^{(\eta_{ncx}-1)FV/RT}\right)} \tag{S11}$$

where $\bar{I}_{ncx}$ is the maximal NCX current, $[Ca^{2+}]_o$ is the extracellular [Ca^{2+}], and $[Na^+]_i$ and $[Na^+]_o$ are the intracellular and extracellular [Na^+], respectively. All other parameters are given in Table S3.

Plasma Membrane Ca^{2+}-ATPase

In addition to NCX the sarcolemma extrudes Ca^{2+} from the cell via a plasma membrane Ca^{2+}-ATPase flux (PMCA) of the form

$$J_{pmca} = \frac{-A_m I_{pmca}}{2FV_{myo}} \tag{S12}$$

$$I_{pmca} = \bar{I}_{pmca}\left(\frac{[Ca^{2+}]_i^{\,2}}{(K_{pmca})^2 + [Ca^{2+}]_i^{\,2}}\right) \tag{S13}$$

where $\bar{I}_{pmca}$ is the maximal PMCA current.

Sarcolemmal Background Ca^{2+} Leak

The sarcolemma includes a constant background Ca^{2+} influx which balances J_{pmca} and J_{ncx} given by

$$J_{bca} = -\frac{A_m I_{bca}}{2FV_{myo}} \tag{S14}$$

$$I_{bca} = g_{bca}(V - E_{ca}) \tag{S15}$$

where g_{bca} is the maximal conductance and E_{ca} is the reversal potential for Ca^{2+},

$$E_{ca} = \frac{RT}{2F}\log\left(\frac{[Ca^{2+}]_o}{[Ca^{2+}]_i}\right) \tag{S16}$$

Total JSR refill and dyadic subspace efflux terms

The total refill flux from the NSR to each JSR compartment includes the contribution from each CRU and is given by

$$J^T_{refill} = \sum_{i=1}^{N} J^i_{refill} = \sum_{i=1}^{N} \frac{v^T_{refill}}{N}([Ca^{2+}]_{nsr} - [Ca^{2+}]^i_{jsr}). \tag{S17}$$

and similarly, the total flux out of the N dyadic subspaces into the bulk myoplasm is given by

$$J^T_{efflux} = \sum_{i=1}^{N} J^i_{efflux} = \sum_{i=1}^{N} \frac{v^T_{efflux}}{N}([Ca^{2+}]^i_{ds} - [Ca^{2+}]_i). \tag{S18}$$

Non-junctional RyR Ca^{2+} Channels

The Ca^{2+} flux from non-junctional or "rogue" RyR Ca^{2+} flux is

$$J_{ryr,nj} = \pi^o_{ryr,nj} v_{ryr,nj}([Ca^{2+}]_{nsr} - [Ca^{2+}]_i). \tag{S19}$$

where $v_{ryr,nj}$ is the total non-junctional RyR release rate in s^{-1} and $\pi^o_{ryr,nj}$ is the fraction of open non-junctional RyRs and solves

$$\frac{d\pi^o_{ryr,nj}}{dt} = \phi k^+(1 - \pi^o_{ryr,nj}) - k^-\pi^o_{ryr,nj} \tag{S20}$$

where $\phi = \phi_m[Ca^{2+}]_{nsr} + \phi_b$, k^+ and k^- are transition rates for a individual RyR as presented in Fig. 1B.

Dynamic Buffering Fractions

Myoplasmic Buffering

Buffering in the myoplasm is approximated using a dynamic buffering fraction given by

$$\beta_{myo} = \left(1 + \frac{B_{myo}^T K_m^{myo}}{(K_m^{myo} + [Ca^{2+}]_i)^2}\right)^{-1} \tag{S21}$$

where B_{myo}^T is the total myoplasmic buffer concentration, K_m^{myo} is the half saturation constant for the myoplasmic buffer.

Junctional SR Buffering

Buffering in each JSR compartment is approximated using a dynamic buffering fraction given by

$$\beta_{jsr}^i = \left(1 + \frac{B_{jsr}^T K_m^{jsr}}{(K_m^{jsr} + [Ca^{2+}]_{jsr}^i)^2}\right)^{-1} \tag{S22}$$

where B_{jsr}^T is the total JSR buffer concentration, K_m^{jsr} is the half saturation constant for the JSR buffer.

Fast Subspace

Similar to previous work (24, 25) model parameters lead to rapid equilibrium of the $[Ca^{2+}]_{ds}$ with the $[Ca^{2+}]_i$ and $[Ca^{2+}]_{jsr}$ (24). Thus, in each dyadic subspace we assume a $[Ca^{2+}]$ ($[Ca^{2+}]_{ds,ss}^i$) that balances the fluxes in and out of that compartment,

$$0 = \frac{\beta_{ds}}{\lambda_{ds}}\left(J_{ryr}^i - J_{efflux}^i\right) = \frac{\beta_{ds}}{\lambda_{ds}}\left(N_o^i v_{ryr}\left([Ca^{2+}]_{jsr}^i - [Ca^{2+}]_{ds}^i\right) - v_{efflux}([Ca^{2+}]_{ds}^i - [Ca^{2+}]_i)\right),$$

that is,

$$[Ca^{2+}]_{ds,ss}^i = \frac{v_{efflux}[Ca^{2+}]_i + N_o^i v_{ryr}[Ca^{2+}]_{jsr}^i}{v_{efflux} + N_o^i v_{ryr}} \tag{S23}$$

where $1 \le i \le N$ and $v_{efflux} = v_{efflux}^T/N$.

Supplemental Figures

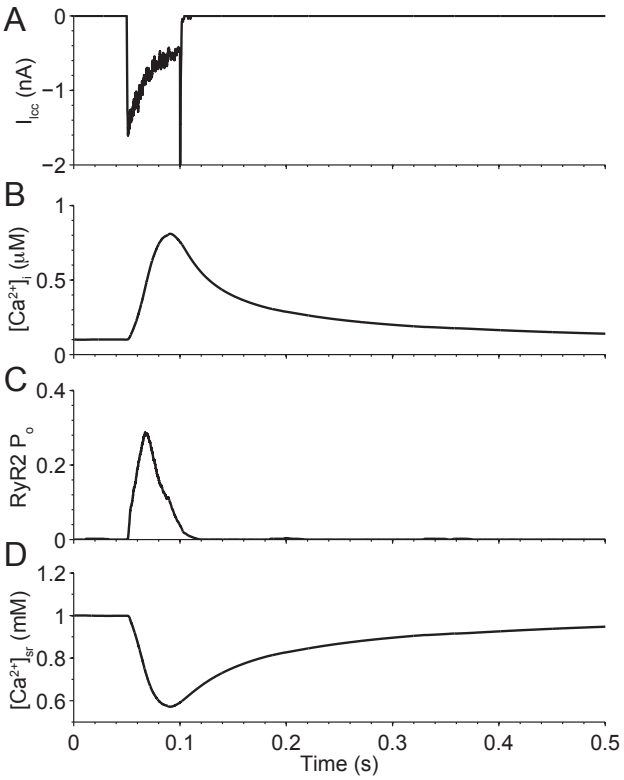

Figure S1: Whole-cell Ca^{2+} handling dynamics (A) LCC current induced from a 50 ms voltage pulse to 10 mV. (B) Bulk myoplasmic $[Ca^{2+}]$ ($[Ca^{2+}]_i$), (C) fraction of open RyRs, and (D) bulk SR $[Ca^{2+}]$ ($[Ca^{2+}]_{nsr}$). Note, $\sim$ 60% of the CRUs are triggered during this simulation and each CRU contains 7 LCCs and 49 RyRs.

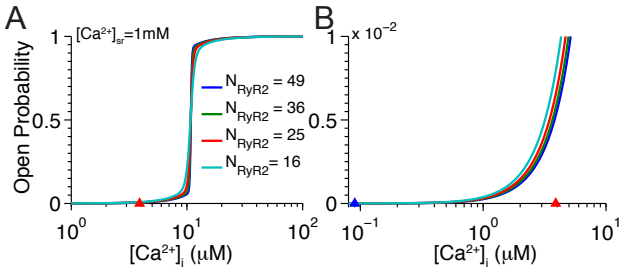

Figure S2: Influence of RyR cluster size (N_{RyR}) on CRU P_o. (A) P_o for a clusters of varying size as a function of $[Ca^{2+}]_i$ and (B) $[Ca^{2+}]_{nsr}$.

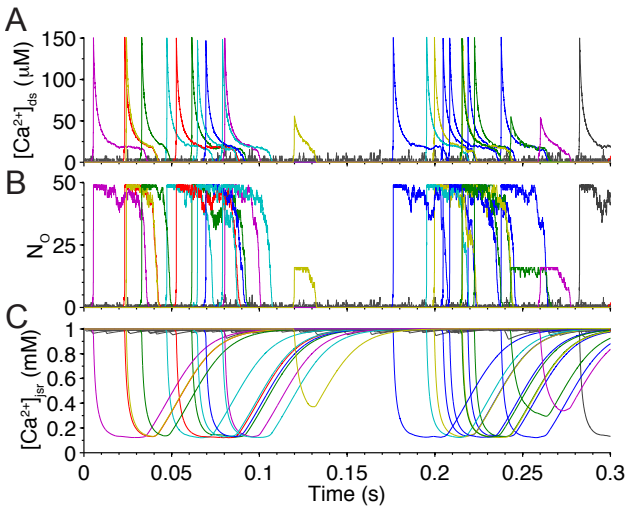

Figure S3: Ca^{2+}spark dynamics with heterogenous cluster size. (A) $[Ca^{2+}]_{ds}$ during spontaneous, diastolic Ca^{2+} release events resulting from clusters of 49 and 16 RyRs . (B) N_o at each CRU. (C) $[Ca^{2+}]_{jsr}$ present on the luminal side of RyR cluster. Each colored line represents a different CRU.

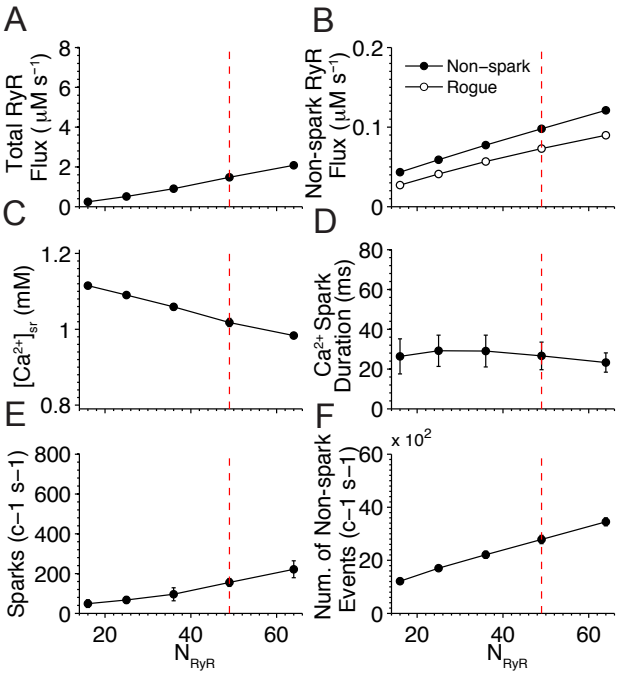

Figure S4: Influence of RyR cluster size (N_{RyR}) on RyR based leak. (A) Total integrated RyR flux during a 1 second simulation, (B) integrated "non-spark" RyR flux via junctional RyRs (*solid line, filled circles*) and non-junctional RyRs (*solid line, open circles*), (C) steady-state $[Ca^{2+}]_{sr}$, (D) average Ca^{2+} spark duration, (E) Ca^{2+} spark rate, and (F) number of "non-spark" events versus $[Ca^{2+}]_{sr}$. The junctional "non-spark" flux is defined as RyR activity that doesn't precede a Ca^{2+} spark. Data points represent the average over 10 simulations and error bars indicate standard deviation from the mean. Note, $[Ca^{2+}]_i$ was held constant at 90 nM.

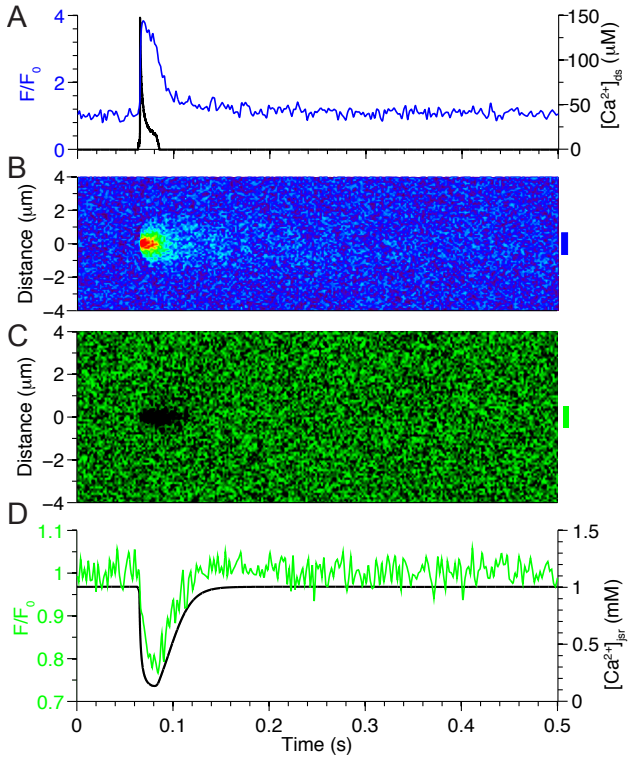

Figure S5: Dynamics of Ca^{2+} sparks and blinks. (A) Time course of $[Ca^{2+}]_{ds}$ and the corresponding fluorescence profile (F/F_0) of Fluo3 (*blue line*). F/F_0 profile was obtained by averaging fluorescence from a 1 μm wide region (*blue box*) in B. (B) Simulated linescan of Ca^{2+} spark. (C) Simulated linescan of Ca^{2+} blink. (D) Time course of $[Ca^{2+}]_{jsr}$ and the corresponding fluorescence profile (F/F_0) of Fluo5N (*blue line*). F/F_0 profile was obtained by averaging fluorescence from a 1 μm wide region (*green box*) in C. Both simulated linescans based on previously published methods (see (16, 40)).

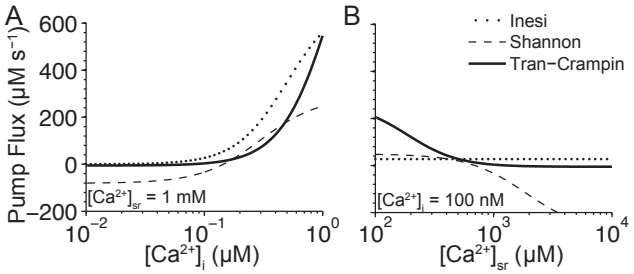

Figure S6: Comparison of SERCA2a pump flux versus (A) $[Ca^{2+}]_i$ and (B) $[Ca^{2+}]_{sr}$ for the three common model formulations; Tran-Crampin (*solid line*) (21), Shannon (*dashed line*) (41), and Inesi (*dotted line*) (42).